

studies are necessary to clarify the contribution of individual alveolar septal cell types. We also understand that the definition of AL, AD, and ADS cells is quite subjective. But we consider this to be the limit of light microscopic studies using fixed time point specimens to observe the potential involvement of septation in compensatory lung growth. Techniques such as real-time lung microscopy will be required to further elucidate the sequential events that may be occurring during the early phase of compensatory lung growth. In addition, not only left pneumonectomy but also positive pressure ventilation may have influenced TTF-1 expression, as the protein level was slightly elevated in the THX group in comparison with the CON group, although statistical significance was not reached.

Evolving knowledge in tissue engineering and regeneration may some day accomplish the assembly of functional lung tissue *ex vivo*. But for the meantime, facilitation of compensatory lung growth in the residual lung may be a more attainable goal to improve residual lung function after resection. Certain pharmacological agents have been reported to increase TTF-1 expression in alveolar cells *in vitro* (29). The results of the present study suggest that lung-specific TTF-1 augmentation, possibly through the airway, may be one candidate for therapeutic facilitation and/or reactivation of compensatory lung growth after lung resection in adult humans. It is intuitively understood that compensatory lung growth requires the synchrony and balance of multiple pathways. Manipulation of transcription factors such as TTF-1 may be influential in that it is capable of regulating multiple pathways simultaneously. But because sustained overexpression of TTF-1 has been shown to impair alveolarization in the postnatal lung (25), it is likely that TTF-1 needs to be finely controlled to appropriately orchestrate the early phase of compensatory lung growth. It is also speculated that the lung stem cell population may exist within the AD and/or the ADS cells (30). Although their potential role in compensatory lung growth may be marginal (31), further research is needed in this area.

In this study, the mouse postpneumonectomy lung growth model was used because of its reliability, reproducibility, and establishment as a model of lung growth. To examine the early phase of compensatory lung growth, we used 9-week-old mice because these mice are mature but are still considered to have high plasticity for postnatal lung growth and/or compensatory lung growth. Conversely, it is true that these mice are still in a growth phase as indicated by the increase in body weight during the experiment; hence, the relevance of this model to adult humans may be limited. Nevertheless, we believe that the present model allows us to effectively dissect potentially new mechanisms into the regulation, and possibly induction, of compensatory lung growth. Further studies in aged mice and other animal species may provide more clinically relevant data regarding the potential induction or facilitation of compensatory lung growth after lung resection in adult humans.

Conflict of Interest Statement: None of the authors has a financial relationship with a commercial entity that has an interest in the subject of this manuscript.

Acknowledgment: The authors thank Hitoshi Abe, Department of Pathology, School of Medicine, Keio University, for his expertise in immunohistochemistry. The authors thank Kei Tsujioaka, Division of General Thoracic Surgery, School of Medicine, Keio University, for her expertise in animal experiments.

References

- Laros CD, Westermann CJ. Dilatation, compensatory growth, or both after pneumonectomy during childhood and adolescence. A thirty-year follow-up study. *J Thorac Cardiovasc Surg* 1987;93:570-576.
- Nakajima C, Kijimoto C, Yokoyama Y, Miyakawa T, Tsuchiya Y, Kuroda T, Nakano M, Saeki M. Longitudinal follow-up of pulmonary function after lobectomy in childhood-factors affecting lung growth. *Pediatr Surg Int* 1988;13:341-345.
- Kriesel D, Krupnick AS, Huddleston CB. Outcomes and late complications after pulmonary resections in pediatric population. *Semin Thorac Cardiovasc Surg* 2004;16:215-219.
- Binns OA, DeLima NF, Buchanan SA, Lopes MB, Cope JT, Marek CA, King RC, Laubach VE, Tribble CG, Kron IL. Mature pulmonary lobar transplants grow in an immature environment. *J Thorac Cardiovasc Surg* 1997;114:186-194.
- Fehrenbach H, Voswinckel R, Michl V, Mehling T, Fehrenbach A, Seeger W, Nyengaard JR. Neoalveolarisation contributes to compensatory lung growth following pneumonectomy in mice. *Eur Respir J* 2008;31:483-485.
- Voswinckel R, Motejl V, Fehrenbach A, Wegmann M, Mehling T, Fehrenbach H, Seeger W. Characterisation of post-pneumonectomy lung growth in adult mice. *Eur Respir J* 2004;24:524-532.
- Kaza AK, Laubach VE, Kern JA, Long SM, Fiser SM, Tepper JA, Nguyen RP, Shockey KS, Tribble CG, Kron IL. Epidermal growth factor augments postpneumonectomy lung growth. *J Thorac Cardiovasc Surg* 2000;120:916-921.
- Sakamaki Y, Matsumoto K, Mizuno S, Miyoshi S, Matsuda H, Nakamura T. Hepatocyte growth factor stimulates proliferation of respiratory epithelial cells during postpneumonectomy compensatory lung growth in mice. *Am J Respir Cell Mol Biol* 2002;26:525-533.
- Kaza AK, Kron IL, Leuwerke SM, Tribble CG, Laubach VE. Keratinocyte growth factor enhances post-pneumonectomy lung growth by alveolar proliferation. *Circulation* 2002;24:1120-1124.
- Sakurai MK, Lee S, Arsenault DA, Nose V, Wilson JM, Heymach JV, Puder M. Vascular endothelial growth factor accelerates compensatory lung growth after unilateral pneumonectomy. *Am J Physiol Lung Cell Mol Physiol* 2007;292:L742-L747.
- Mason RJ. Hepatocyte growth factor: the key to alveolar septation? *Am J Respir Cell Mol Biol* 2002;26:517-520.
- Stahlman MT, Gray ME, Whitsett JA. Expression of thyroid transcription factor-1 (TTF-1) in fetal and neonatal human lung. *J Histochem Cytochem* 1996;44:673-678.
- Yang MC, Guo Y, Liu CC, Weissler JC, Yang YS. The TTF-1/TAP26 complex differentially modulates surfactant protein-B (SP-B) and -C (SP-C) promoters in lung cells. *Biochem Biophys Res Commun* 2006;344:484-490.
- Scherle W. A sample method for volumetry of organs in quantitative stereology. *Mikroskopie* 1970;26:57-60.
- Weibel ER. Stereological methods. In: E. R. Weibel, ed. Practical methods for biological morphometry. London: Academic Press; 1979.
- Kawakami M, Paul JL, Thurlbeck WM. The effect of age on lung structure in male BALB/cNnia inbred mice. *Am J Anat* 1984;170:1-21.
- Inselman LS, Pedilla-Burgos LB, Teichberg S, Spencer H. Alveolar enlargement in obesity-induced hyperplastic lung growth. *J Appl Physiol* 1988;65:2291-2296.
- Massaro D, Massaro GD, Clerch LB. Noninvasive delivery of small inhibitory RNA and other reagents to pulmonary alveoli in mice. *Am J Physiol Lung Cell Mol Physiol* 2004;287:L1066-L1070.
- Li C, Cai J, Pan Q, Minoo P. Two functionally distinct forms of Nkx2.1 protein are expressed in pulmonary epithelium. *Biochem Biophys Res Commun* 2000;270:462-468.
- Kimura S. Thyroid-specific enhancer-binding protein role in thyroid function and organogenesis. *Trends Endocrinol Metab* 1996;7:247-252.
- Minoo P, Su G, Drum H, Bringas P, Kimura S. Defects in tracheoesophageal and lung morphogenesis in Nkx2.1(-/-) mouse embryos. *Dev Biol* 1999;209:60-71.
- Kelly SE, Bachurski CJ, Baurhans MS, Glasser SW. Transcription of the lung-specific surfactant protein C gene is mediated by thyroid transcription factor 1. *J Biol Chem* 1996;271:6881-6888.
- Berger LC, Burri PH. Timing of the quantitative recovery in the regenerating rat lung. *Am Rev Respir Dis* 1985;132:777-783.
- Brown LM, Rannels SR, Rannels DE. Implications of post-pneumonectomy lung growth in pulmonary physiology and disease. *Respir Res* 2001;2:340-347.
- Wert SE, Dey CR, Blair PA, Kimura S, Whitsett JA. Increased expression of thyroid transcription factor-1 (TTF-1) in respiratory epithelial cells inhibits alveolarization and causes pulmonary inflammation. *Dev Biol* 2002;242:75-87.
- Mitani A, Nagase T, Fukuchi K, Aburatani H, Makita R, Kurihara H. Transcriptional coactivator with PDZ-binding motif is essential for

- normal alveolarization in mice. *Am J Respir Crit Care Med* 2009;180:326–338.
27. Kurotani R, Tomita T, Yang Q, Carlson BA, Chen C, Kimura S. Role of secretoglobin 3A2 in lung development. *Am J Respir Crit Care Med* 2008;178:389–398.
28. Hsia CC, Johnson RL Jr. Further examination of alveolar septal adaptation to left pneumonectomy in the adult lung. *Respir Physiol Neurobiol* 2006;151:167–177.
29. Kolla V, Gonzales LW, Gonzales J, Wang P, Angampalli S, Feinstein SI, Ballard PL. Thyroid transcription factor in differentiating type II cells: regulation, isoforms, and target genes. *Am J Respir Cell Mol Biol* 2006;36:213–225.
30. Giangreco A, Reynolds SD, Stripp BR. Terminal bronchioles harbor a unique airway stem cell population that localizes to the bronchoalveolar duct junction. *Am J Pathol* 2002;161:173–182.
31. Nolen-Walston RD, Kim CF, Mazan MR, Ingenito EP, Gruntman AM, Tsai L, Boston R, Woolfenden AE, Jacks T, Hoffman AM. Cellular kinetics and modeling of bronchioalveolar stem cell response during lung regeneration. *Am J Physiol Lung Cell Mol Physiol* 2008;294:L1158–L1165.

Case Reports

A Non-invasive Thymoma that Occurred 29 Years After Complete Resection of a Non-invasive Thymoma Accompanied by a Microthymoma

Yoshikane Yamauchi^{1,*}, Mitsutomo Kohno¹, Tai Hato¹, Yuichiro Hayashi², Yotaro Izumi¹ and Hiroaki Nomori¹

¹Department of Surgery, School of Medicine, Keio University and ²Department of Pathology, School of Medicine, Keio University, Tokyo, Japan

*For reprints and all correspondence: Yoshikane Yamauchi, Department of Surgery, School of Medicine, Keio University, 35 Shinanomachi, Shinjuku-ku, Tokyo 160-8582, Japan. E-mail: yoshikaney@2004.jukuin.keio.ac.jp

Received October 11, 2009; accepted April 10, 2010

A 55-year-old woman with a 7 cm non-invasive thymoma and myasthenia gravis had been treated by extended thymectomy via median sternotomy 29 years ago. A microscopic 0.15 cm thymoma (microthymoma) was incidentally found in the thymus during surgery. Twenty-nine years later, a 5 cm thymoma developed in the anterior mediastinum and was surgically treated. The non-invasive first thymoma, the microthymoma and the non-invasive third thymoma were all classified as type AB thymomas according to the World Health Organization (WHO) classification and showed extremely similar histological findings. We think the mechanism underlying the local recurrence of non-invasive thymomas would be intrathymic metastasis because of their clinical and pathological features.

Key words: thymoma – local recurrence – multicentric development – intrathymic metastasis – microthymoma

INTRODUCTION

Thymoma is a low-grade malignant tumor generally associated with a good prognosis after surgical treatment. However, in the case of non-invasive thymomas, there is a 1.3–5.4% chance of local recurrence even after complete resection (1–3). Local recurrence after complete resection of non-invasive thymomas has been reported to be caused by multicentric development of thymomas (1). In 1990, we reported the case of a 26-year-old woman with two synchronous thymomas: (i) a non-invasive thymoma that was 7 cm in size and (ii) a microscopic thymoma (microthymoma) that was 0.15 cm in size (4). Twenty-nine years later, the patient developed another thymoma, which was again treated by surgical resection. Here, we discuss the mechanism underlying the development of these 3 thymomas by comparing their histological findings.

CASE REPORT

The patient was a 55-year-old woman. At the age of 26 years, she had undergone extended thymectomy via median

sternotomy for a non-invasive thymoma and generalized myasthenia gravis (MG). The thymoma was 7 cm in size; a 0.15 cm well-encapsulated microthymoma was incidentally found in the thymus. The histological features of the microthymoma were quite similar to those of the larger tumor, which was reported by one of our coauthors (H.N.) in 1990 (4). Because the symptoms of MG diminished soon after surgery, she decided to stop visiting us.

In October 2008, 29 years after the initial treatment, she complained of general fatigue again. Chest computed tomography revealed an anterior mediastinal mass 5 cm in size (Fig. 1). Although the result of the tensilon test was negative, the serum anti-acetylcholine receptor antibody (anti-achR Ab) level was elevated to 41 nmol/l. In December 2008, the tumor was resected via left thoracotomy. The tumor was located at the anterolateral side of the aortic arch, anterior to the phrenic nerve and adjacent to the sternum, pericardium and upper lobe of the left lung. The tumor was resected concomitant with wedge resection of the upper lobe of the left lung (Fig. 2). Pathological examination revealed a fibrous thick wall totally covering the tumor; the diagnosis was a

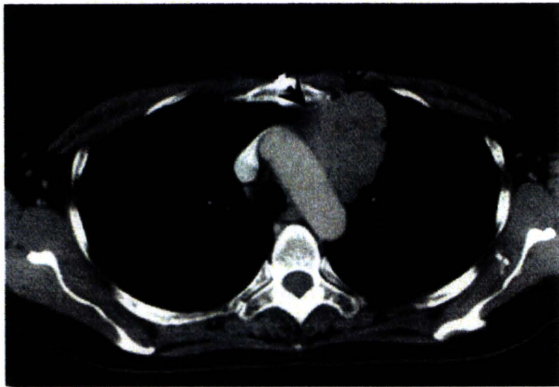


Figure 1. Computed tomography performed 29 years after the first surgery, showing a well-defined mass in the anterior mediastinum, adjacent to the aortic arch. The arrows indicate the margin of the tumor.

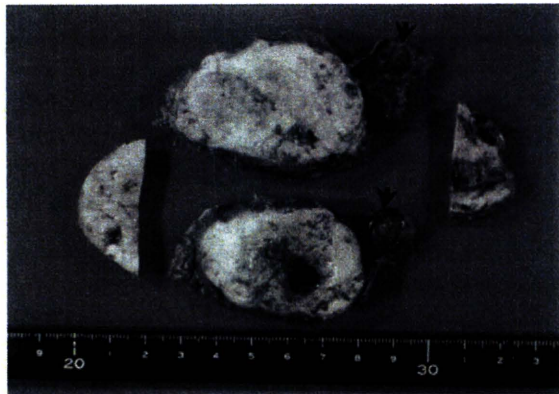


Figure 2. Anterior mediastinal tumor resected in the second surgery, in which wedge resection of the upper lobe of the left lung (arrow) was also performed.

non-invasive thymoma of histological type AB. Capsular invasion was not observed microscopically or macroscopically. The histological features of the tumor were quite similar to those of the two thymomas that were detected 29 years ago (Fig. 3).

Although her post-operative clinical course was fair, her general fatigue did not improve because of the elevation of the serum level of anti-achR Ab up to 170 nmol/l. Her condition was not symptomatic enough for MG to be diagnosed, but the induction of pyridostigmine bromide therapy significantly improved her symptoms. To date (i.e. 1 year after the second surgery), she has remained healthy and asymptomatic and is on oral pyridostigmine bromide therapy.

DISCUSSION

The recurrence rate of non-invasive thymomas after resection has been reported to be 1.3–5.4% (1–3); the tumor sometimes recurs many years after complete resection because of its slow growth rate. Awad et al. (4) reported a case of local recurrence of non-invasive thymoma 37 years after complete resection of the tumor. Nomori et al. (5) reported a case in which non-invasive thymoma developed over 20 years before it was detected; the patient developed pulmonary metastases 12 years after it had been resected, resulting in a 32-year clinical course.

The mechanism underlying the local recurrence of non-invasive thymomas is controversial, but the following mechanisms have been posited: (i) local recurrence at the surgical margin; (ii) lymph node metastasis; (iii) multicentric development of thymomas in the remnant thymic tissue; and (iv) intrathymic metastasis in the remnant thymic tissue. Because all the thymomas in this patient were non-invasive, the possibility of local recurrence at the surgical margin can be

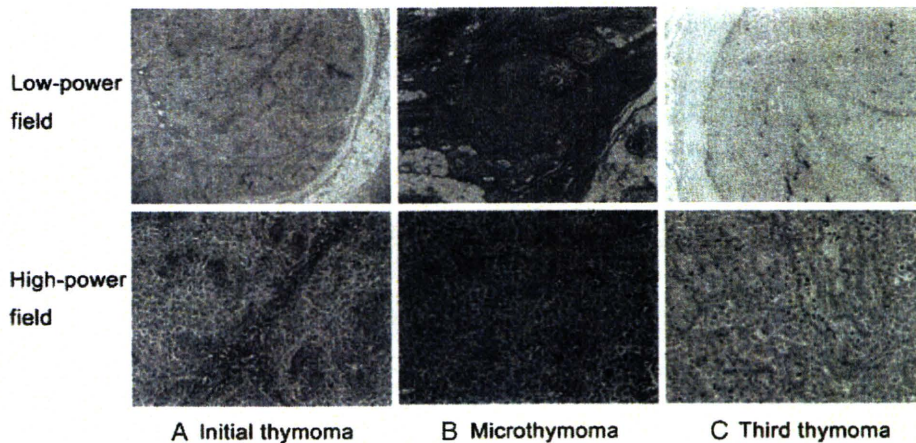


Figure 3. Comparison of the histological findings of the specimens obtained from the two surgeries. (a) Non-invasive thymoma obtained during the initial resection. (b) Microthymoma obtained during the initial resection. (c) Non-invasive thymoma obtained during the second resection. The tumors were solid and consisted of thymic epithelial cells with abundant cytoplasm, round-to-oval-shaped vesicular nuclei and inconspicuous nucleoli with a strand-like pseudo-glandular structure (low-power field: H&E, ×10; high-power field: H&E, ×100). A few lymphocytes are scattered among the epithelial cells. The histological findings were very similar for the three tumors.

excluded, although it is hard to determine whether multicentric development or the intrathymic metastasis caused the development of multiple thymomas. We could not exclude the possibility that the third thymoma occurred because of lymph node metastasis. However, thymomas rarely metastasize to the lymph nodes, and lymph node metastasis has not occurred in this patient to date. Moreover, the recurrent tumor did not exhibit any histological structures characteristic of lymph node tissue. Therefore, the third tumor may not be a lymph node metastasis. Mori et al. (6) reviewed the histological types of thymomas in 12 patients with multiple thymomas, including 3 of their own patients, and reported that 10 patients (83%) had the same histological subtypes. Although they concluded that most multiple thymomas might develop from identical tumorigenesis, we prefer the hypothesis that intrathymic metastasis caused the development of multiple thymomas in the present case for the following reasons: (i) all the thymomas exhibited extremely similar histological features; (ii) the sizes of the two thymomas detected initially were significantly different (i.e. 7 cm and 0.15 cm), suggesting the possibility that the smaller tumor was an intrathymic metastasis; and (iii) it is quite likely that the third thymoma originated from the intrathymic microscopic metastasis and grew gradually over 29 years because thymomas are characterized by slow growth (4–5). Even though this patient initially underwent extended thymectomy, microscopic thymic tissue could have remained because the distribution of thymic tissue is extensive and complicated (7–8).

Another important issue in the present case is the occurrence of the microthymoma, which was found incidentally in the thymus 29 years ago. The term ‘microthymoma’ was first proposed for microscopic thymomas by Cheuk et al. (9) in 2005. Mori et al. (10) reviewed seven patients with microthymomas, including three of their own patients and the present case when it was initially reported in 1990. Those microthymomas ranged from 0.15 to 0.7 cm in size, with our patient’s microthymoma being the smallest one. The findings for our patient suggest that the occurrence of microthymomas is a risk factor for the recurrence of non-invasive thymomas.

In our patient, because the third tumor was located anterior to the phrenic nerve, it is possible that it might have

developed from remnant thymic tissue after the first surgery, even though an extended thymectomy had been performed. Surgeons must exercise great caution to not leave any remnants of thymic tissue while performing extended thymectomy; not to mention that mere extirpation of the tumor is inadequate in the case of thymomas, even if the tumor is encapsulated.

Therefore, while treating thymomas, it is very important not only to perform a ‘complete’ extended thymectomy but also to perform pathological tests on thin slices of thymic tissue for detecting microthymomas. For patients with microthymoma, a lengthy follow-up (more than 20 years) is essential to determine a local recurrence.

Conflict of interest statement

None declared.

References

- Bernatz PE, Harrison EG, Clagett OT. Thymoma: a clinicopathologic study. *J Thorac Cardiovasc Surg* 1961;42:424–44.
- Masaoka A, Monden Y, Nakahara K, Tanioka T. Follow-up study of thymomas with special reference to their clinical stages. *Cancer* 1981;48:2485–92.
- Strobel P, Baur A, Puppe B, Kraushaar T, Krcin A, Toyka K, et al. Tumor recurrence and survival in patients treated for thymomas and thymic squamous cell carcinomas: a retrospective analysis. *J Clin Oncol* 2004;22:1501–9.
- Awad WJ, Symmans PJ, Dussek JE. Recurrence of stage I thymoma 32 years after total excision. *Ann Thorac Surg* 1998;66:2106–8.
- Nomori H, Kobayashi K, Ishihara T, Suito T, Torikata C. A case of multiple thymoma: the possibility of intra-thymic metastasis. *Jpn J Clin Oncol* 1990;20:209–11.
- Mori T, Nomori H, Ikeda K, Yoshioka M, Kobayashi H, Iwatani K, et al. Three cases of multiple thymoma with a review of the literature. *Jpn J Clin Oncol* 2007;37:146–9.
- Jaretzki A, 3rd, Wolff M. ‘Maximal’ thymectomy for myasthenia gravis. Surgical anatomy and operative technique. *J Thorac Cardiovasc Surg* 1988;96:711–6.
- Masaoka A, Yamakawa Y, Niwa H, Fukai I, Kondo S, Kobayashi M, et al. Extended thymectomy for myasthenia gravis patients: a 20-year review. *Ann Thorac Surg* 1996;62:853–9.
- Cheuk W, Tsang WY, Chan JK. Microthymoma: definition of the entity and distinction from nodular hyperplasia of the thymic epithelium (so-called microscopic thymoma). *Am J Surg Pathol* 2005;29:415–9.
- Mori T, Nomori H, Ikeda K, Kobayashi H, Iwatani K, Yoshioka M, et al. Microscopic-sized ‘microthymoma’ in patients with myasthenia gravis. *Chest* 2007;131:847–9.

References

1. Beghetti M, Gow RM, Haney I, et al. Pediatric primary benign cardiac tumors: a 15-year review. *Am Heart J* 1997;134:1107-14.
2. Burke AP, Rosado-de-Christenson M, Templeton PA, et al. Cardiac fibroma: clinicopathologic correlates and surgical treatment. *J Thorac Cardiovasc Surg* 1994;108:862-70.
3. Valente M, Cocco P, Thiene G, et al. Cardiac fibroma and heart transplantation. *J Thorac Cardiovasc Surg* 1993;106:1208-12.
4. Meissner C, Minnasch P, Gafumbegete E, et al. Sudden unexpected infant death due to fibroma of the heart. *J Forensic Sci* 2000;45:731-3.
5. Stiller B, Hetzer R, Meyer R, et al. Primary cardiac tumors: when is surgery necessary? *Eur J Cardiothorac Surg* 2001;20:1002-6.
6. Bapat VN, Varma GG, Hardikar AA, et al. Right ventricular fibroma presenting as tricuspid stenosis—case report. *Thorac Cardiovasc Surg* 1996;44:152-4.

Mediastinal Germ Cell Tumor With Somatic-Type Malignancy: Report of 5 Stage I/II Cases

Keisuke Asakura, MD, Yotaro Izumi, MD, PhD,
Tatsuhiko Ikeda, MD, Yoshishige Kimura, MD,
Hirohisa Horinouchi, MD, PhD, Yuichiro Hayashi, MD,
and Hiroaki Nomori, MD, PhD

Division of General Thoracic Surgery, and Department of Pathology, School of Medicine, Keio University, Tokyo, Japan

Among 15 patients with primary mediastinal nonseminomatous germ cell tumors experienced during the past 12 years, 5 were diagnosed with germ cell tumors with somatic-type malignancy. The pretreatment stages were stage I in 2 patients and stage II in 3. All 5 patients received perioperative chemotherapy plus surgical resection, and 4 remain alive without relapse, with a mean follow-up of 60 months.

(Ann Thorac Surg 2010;90:1014-6)

© 2010 by The Society of Thoracic Surgeons

A germ cell tumor with somatic-type malignancy (GCT-STM) is a germ cell tumor (GCT) accompanied by somatic-type malignant (STM) components, such as sarcoma, carcinoma, or both, according to the most recent histologic classification of the World Health Organization [1]. The GCT-STM reportedly accounts for 11% to 29% of all cases of mediastinal GCT in adults [2-4] and is mostly diagnosed from resected specimens. There have also been reports made that patients who have GCT-STM are generally diagnosed at an advanced stage and are resistant to chemotherapy with poor prognoses (mean survival time, 14 to 15 months) [2-6]. An extended case report on stage I-II GCT-STM patients is rare.

Accepted for publication Dec 30, 2009.

Address correspondence to Dr Izumi, Division of General Thoracic Surgery, Department of Surgery, School of Medicine, Keio University, 35 Shinanomachi, Shinjuku-ku, Tokyo, 160-8582, Japan; e-mail: yotarozumi@a2.keio.jp.

Fifteen patients with mediastinal nonseminomatous GCT were treated with chemotherapy or radiotherapy, or both, plus surgical treatment in Keio University Hospital between 1995 and 2007. Of these, 15 patients, 5 were histologically diagnosed as GCT-STM from the resected specimens. Diagnoses of GCT-STM were made according to morphologic criteria previously described, and STM components that lacked expansile and invasive growth patterns, which were excluded from the GCT-STM diagnoses [6]. Clinical staging was based on Moran and Suster's [2] staging scheme.

Table 1 summarizes the clinicopathologic features of the 5 patients. The serum α -fetoprotein levels were elevated in all 5 patients before initial treatment. All patients, except patient 1, had undergone chemotherapy before surgery, complemented by a bleomycin, etoposide, cisplatin (BEP) regimen of two to four courses. Patient 1 had first undergone surgical resection at another institution. No STM component was found in the resected specimen. The BEP regimen was done after surgery. Patient 1 presented with local recurrence without serum α -fetoprotein elevation at 7 months after the initial resection; the patient was referred to our institution. Radiologic responses to BEP therapy were progressive disease in patient 1 and no change in the other 4 patients. Serum α -fetoprotein levels decreased to a normal range (0 to 20 ng/mL) in all patients. All 5 patients were treated by complete resection (re-resection in patient 1). The resected specimens showed variable STM components, such as angiosarcoma, glioma, leiomyosarcoma, rhabdomyosarcoma, liposarcoma, osteosarcoma, chondrosarcoma, malignant fibrous histiocytoma, and adenocarcinoma (Table 1, Fig 1). Patient 1 underwent radiation therapy (50 Gy) after re-resection. Patients 2 and 4 had undergone postoperative chemotherapy, with one and three courses, respectively, of a BEP regimen. Of the 5 patients, 4 are alive and without recurrence, between 27 and 132 months after initial treatment. Patient 5 died of disease 19 months after treatment. A needle biopsy for multiple liver metastases in this patient showed metastasis of leiomyosarcoma.

Comment

It has been reported that it is very difficult to diagnose GCT-STM from biopsy specimens, and that such a diagnosis can only be made from resected specimens, typically after chemotherapy [4, 5, 7, 8]. Although Athanasiou and colleagues [8] retrospectively reported that computed tomographic or magnetic resonance imaging findings, or both, in 6 of 14 patients with GCT-STM could indicate the presence of STM components, those findings were of particular types of STM components, such as osteosarcoma showing expanded ossification, adenocarcinoma showing cancerous peritonitis, or bronchioloalveolar carcinoma showing an expanded pulmonary ground-glass opacity-like appearance. However, other STM components would not be easily detected on either computed tomographic or magnetic resonance imaging.

From our present series of patients, we speculate that one characteristic clinical finding of GCT-STM may be a minimal reduction or even an increase in tumor size after

Table 1. Clinicopathologic Features of 5 Germ Cell Tumor Somatic Type Malignancy Cases

Patient No.	Age/Sex	Final Histology		Stage	BEP	Tumor Size (cm)		α-Fetoprotein (ng/mL)		Outcome
		GCT	STM			Before	After	Before	After	
1	24/M	MT	AC	II	3	0 ^a	6	3	3	Alive: 132 months
2	21/M	IT, YT	RMS	I	3	6	5	304	5	Alive: 89 months
3	35/M	MT	AS, GL, OS, CS, LS	I	2	13		197	6	Alive: 36 months
4	34/M	IT	MFH, US	II	2	7	8	377	2	Alive: 27 months
5	45/M	MT	GB, LMS, AC	II	4	15	15	27,600	11	Dead: 19 months

^a Primary resection was done prior to initial chemotherapy.

After = after initial chemotherapy; AC = adenocarcinoma; AS = angiosarcoma; Before = before initial chemotherapy; BEP = courses of bleomycin, etoposide, cisplatin regimen; CS = chondrosarcoma; GB = glioblastoma; GCT = germ cell tumor; GL = glioma; IT = immature teratoma; LMS = leiomyosarcoma; LS = liposarcoma; M = male; MFH = malignant fibrous histiocytoma; MT = mature teratoma; OS = osteosarcoma; RMS = rhabdomyosarcoma; STM = somatic type malignancy; US = unclassified sarcoma; YT = yolk sac tumor.

chemotherapy, despite a normalization of tumor markers. During the same period as the present series, 10 patients presented with primary mediastinal nonseminomatous GCT without STM components. Tumor markers were normalized in 8 of 9 patients who received chemotherapy before resection. Radiologic responses in these 8 patients were complete response in 1, partial response in 3, and no change in 4. In the present series, discrepancies between serum tumor marker response and radiologic response seem to be more common among GCT-STM patients.

There was no STM component in the primary resected specimen of patient 1. The GCT-STM was diagnosed from the re-resected specimen at relapse after chemotherapy. Therefore, it can be speculated that postoperative chemotherapy may have induced the formation of STM component in patient 1. The majority of reports, including our case

series, suggest that chemotherapy or radiotherapy may induce the formation of STM component from the malignant transformation of pre-existing teratoma or the induction of differentiation among the pluripotent germ cell components [6, 8], or both. However, no conclusions can be drawn because primary tumor resection is not usually done in this group of patients.

The GCT-STM has been reported to be generally advanced at diagnosis [8], highly metastatic [5], resistant to standard cisplatin-based chemotherapy [5-7], and associated with poorer prognosis than GCT without STM (the reported mean survival time, 14 to 15 months) [2-6]. In our present series of 5 patients with stage I-II GCT-STM, the mean survival time was 60 months. During the same period, 10 patients with primary mediastinal nonseminomatous GCT without STM components underwent surgical

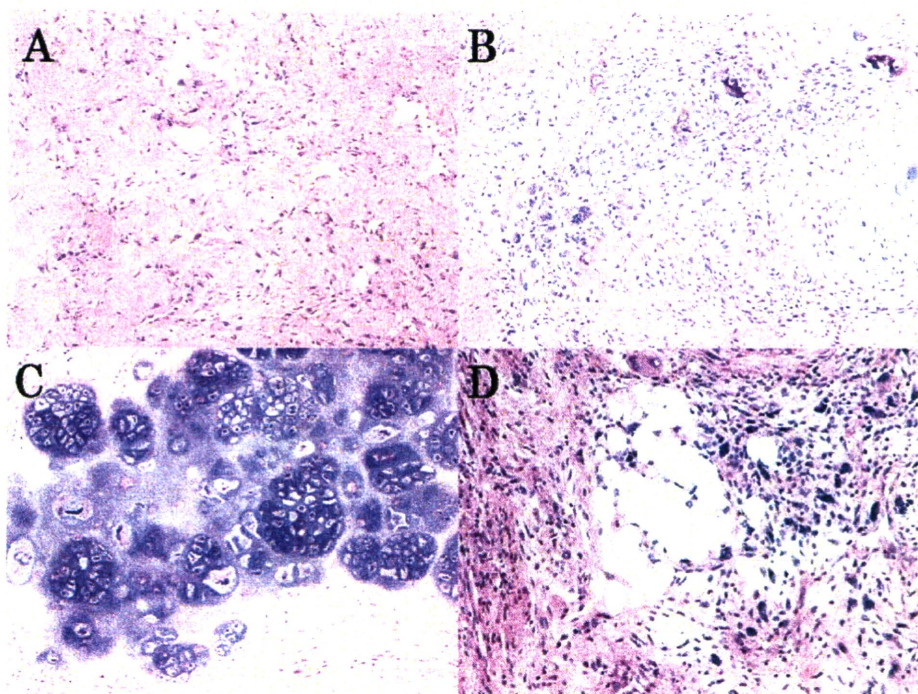


Fig 1. Germ cell tumor with somatic-type malignancy (patient 3). (A) Angiosarcoma component. (Hematoxylin and eosin, ×400.) (B) Osteosarcoma component. (Hematoxylin and eosin, ×400.) (C) Chondrosarcoma component. (Hematoxylin and eosin, ×400.) (D) Liposarcoma component. (Hematoxylin and eosin, ×400.)

resection with perioperative BEP therapy at our institution. Their clinical stages were stage I in 2 patients, stage II in 5, and stage III in 3. The mean survival time of the 7 patients with stage I-II GCT without STM was 84 months, which was not statistically different in comparison with the 5 cases of stage I-II GCT-STM ($p = 0.85$). Prognosis in our 5 patients with GCT-STM was better than previously reported [2-6]. Although most reports do not show the information on clinical stages, Malagon and colleagues [5] reported that clinical stages among 23 patients with mediastinal GCT-STM were stage II in 3 patients, stage III in 15, and unknown in 5. We believe that the specific prognosis of stage I-II mediastinal GCT-STM has not been reported; however, the prognosis may be comparable with stage I-II GCT without STM.

References

1. Travis WD, Muller-Hermelink HK, Harris CC. World Health Organization classification of tumors, pathology and genetics of tumors of the lung, pleura, thymus and heart, 1st ed. Lyon, France: IARC Press; 2004.
2. Moran CA, Suster S. Primary germ cell tumors of the mediastinum: I. Analysis of 322 cases with special emphasis on teratomatous lesions and a proposal for histopathologic classification and clinical staging. *Cancer* 1997;80:681-90.
3. Wright CD, Kesler KA, Nichols CR, et al. Primary mediastinal nonseminomatous germ cell tumors. Results of a multimodality approach. *J Thorac Cardiovasc Surg* 1990;99:210-7.
4. Gonzalez-Vela JL, Savage PD, Manivel JC, Torkelson JL, Kennedy BJ. Poor prognosis of mediastinal germ cell cancers containing sarcomatous components. *Cancer* 1990;66:1114-6.
5. Malagon HD, Valdez AM, Moran CA, Suster S. Germ cell tumors with sarcomatous components: a clinicopathologic and immunohistochemical study of 46 cases. *Am J Surg Pathol* 2007;31:1356-62.
6. Ulbright TM, Loehrer PJ, Roth LM, Einhorn LH, Williams SD, Clark SA. The development of non-germ cell malignancies within germ cell tumors. A clinicopathologic study of 11 cases. *Cancer* 1984;54:1824-33.
7. Donadio AC, Motzer RJ, Bajorin DF, et al. Chemotherapy for teratoma with malignant transformation. *J Clin Oncol* 2003; 21:4285-91.
8. Athanasiou A, Vanel D, El Mesbahi O, Theodore C, Fizaki K. Non-germ cell tumours arising in germ cell tumours (teratoma with malignant transformation) in men: CT and MR findings. *Eur J Radiol* 2009;69:230-5.

Extraskeletal Ewing's Sarcoma Presenting as a Mediastinal Mass

Jane Halliday, MB BChir,
Sing Yang Soon, MB ChB, MRCS,
Hannah Monaghan, MB BS,
William S. Walker, MB BChir, FRCS, and
Vipin Zamvar, MBBS, FRCS

Department of Cardiothoracic Surgery, Royal Infirmary of Edinburgh, Edinburgh, United Kingdom

Ewing's sarcoma family of tumors is part of a rare group of malignant neoplasms with small blue, round-cell

Accepted for publication Jan 13, 2010.

Address correspondence to Dr Halliday, Department of Cardiothoracic Surgery, Royal Infirmary of Edinburgh, 51 Little France Crescent, Old Dalkeith Rd, Edinburgh, EH16 4SA, United Kingdom; e-mail: jane.halliday@cantab.net.

morphology on hematoxylin and eosin stain, expressing CD99, C-Kit, and Bcl2, and sharing the presence of the translocation t(11:22). Extraskeletal Ewing's sarcoma is a rare disease that typically involves the soft tissues of the trunk or extremities. We describe a case of extraskeletal Ewing's sarcoma presenting as a mediastinal mass in a 16-year-old boy.

(Ann Thorac Surg 2010;90:1016-7)

© 2010 by The Society of Thoracic Surgeons

The Ewing's family of tumors are a group of nonhereditary small, blue, round-cell tumors occurring in bone and soft tissues, characterized as a group by the presence of the translocation t(11; 22) (q24; q12). They typically occur in children and young adults, and the majority are osseous in origin. Extraskeletal Ewing's sarcoma is a soft-tissue primary tumor that typically presents as a painful rapidly growing tumor in the lower limb and paravertebral regions.

A 16-year-old boy presented with a 2-day history of dyspnea and stridor at rest. Prior to this acute deterioration he admitted to 6 months intermittent dysphonia and 3 months progressive dyspnea on exertion. He had no other symptoms. On examination he had marked stridor, no lymphadenopathy, and no superior vena cava obstruction. His peak expiratory flow rate was 180 L/min. A right vocal cord palsy was noted during a flexible endoscopy. A chest roentgenogram and computed tomographic scan demonstrated a large upper mediastinal mass with tracheal compression to 5 mm (Fig 1). Thyroid function tests, lactate dehydrogenase, and tumor markers (α -fetoprotein and β -human chorionic gonadotrophin) were normal. An attempted biopsy through a right neck dissection was inconclusive due to sampling error. We elected to perform a right thoracotomy to resect the tumor. Double lumen endotracheal intubation was uneventful. At thoracotomy, we found a large mass in the right paratracheal region. The mass extended from the superior edge of the azygos vein to the thoracic inlet superiorly. Anteroposteriorly it covered the entire apical thoracic cavity. The pleura over the mass were incised. The mass was covered with a capsule and could be

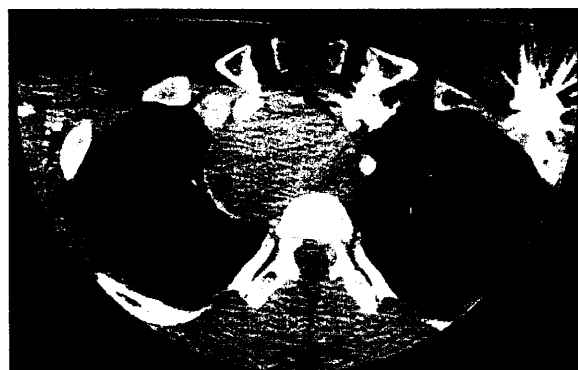


Fig 1. Computed tomographic scan of the thorax in the coronal plane. A large anterior mediastinal mass is demonstrated with maximum axial dimensions of 6.5×4.7 cm and craniocaudal extension of 7.6 cm. The trachea is significantly compressed measuring 5 mm in its mid-portion.

Airway administration of dexamethasone, 3'-5'-cyclic adenosine monophosphate, and isobutylmethylxanthine facilitates compensatory lung growth in adult mice

Yusuke Takahashi, Yotaro Izumi, Mitsutomo Kohno, Masafumi Kawamura, Eiji Ikeda and Hiroaki Nomori

Am J Physiol Lung Cell Mol Physiol 300:L453-L461, 2011. First published 17 December 2010;
doi:10.1152/ajplung.00100.2010

You might find this additional info useful...

This article cites 34 articles, 24 of which can be accessed free at:

<http://ajplung.physiology.org/content/300/3/L453.full.html#ref-list-1>

Updated information and services including high resolution figures, can be found at:

<http://ajplung.physiology.org/content/300/3/L453.full.html>

Additional material and information about *AJP - Lung Cellular and Molecular Physiology* can be found at:

<http://www.the-aps.org/publications/ajplung>

This information is current as of April 18, 2011.

Airway administration of dexamethasone, 3'-5'-cyclic adenosine monophosphate, and isobutylmethylxanthine facilitates compensatory lung growth in adult mice

Yusuke Takahashi,¹ Yotaro Izumi,¹ Mitsutomo Kohno,¹ Masafumi Kawamura,¹ Eiji Ikeda,² and Hiroaki Nomori¹

¹Division of General Thoracic Surgery, Department of Surgery, School of Medicine, Keio University, Tokyo, Japan; and ²Department of Pathology, Yamaguchi University Graduate School of Medicine, Yamaguchi, Japan

Submitted 29 March 2010; accepted in final form 17 December 2010

Takahashi Y, Izumi Y, Kohno M, Kawamura M, Ikeda E, Nomori H. Airway administration of dexamethasone, 3'-5'-cyclic adenosine monophosphate, and isobutylmethylxanthine facilitates compensatory lung growth in adult mice. *Am J Physiol Lung Cell Mol Physiol* 300: L453–L461, 2011. First published December 17, 2010; doi:10.1152/ajplung.00100.2010.—The combination of dexamethasone, 8-bromo-3'-5'-cyclic adenosine monophosphate, and isobutylmethylxanthine, referred to as DCI, has been reported to optimally induce cell differentiation in fetal lung explants and type II epithelial cells. DCI administration is also known to modulate the expression levels of many genes known to be involved in the facilitation of lung growth. Recently, we found that RNA silencing of thyroid transcription factor 1 (TTF-1) delayed compensatory lung growth. DCI is also known to induce TTF-1 expression in pulmonary epithelial cells. From these findings, we hypothesized that DCI administration may facilitate compensatory lung growth. In the present study, using a postpneumectomy lung growth model in 9-wk-old male mice, we found that compensatory lung growth was significantly facilitated by airway administration of DCI immediately following left pneumectomy, as indicated by the increase in the residual right lung dry weight index. TTF-1 expression was significantly elevated by DCI administration, and transient knockdown of TTF-1 attenuated the facilitation of compensatory lung growth by DCI. These results suggested that DCI facilitated compensatory lung growth, at least in part, through the induction of TTF-1. Morphological analyses suggested that DCI administration increased the number of alveoli, made each of them smaller, and produced a net increase in the calculated surface area of the alveoli per volume of lung. The effect of a single administration was maintained during the observation period, which was 28 days. DCI with further modifications may provide the material to potentially augment residual lung function after resection.

thyroid transcription factor 1; wheel-running test; lung function

IT IS GENERALLY ACCEPTED IN the clinic that after lung resection in adults, the residual lung increases in volume to some extent, but that this increase is primarily hyperinflation with minimal recovery, and possibly even deterioration in lung function (16). In contrast, compensatory lung growth after lung resection has been reported in children (24) and in many animal models, including mice (7, 33). While this compensatory lung growth potential may be completely lost in the adult human lung, there is also evidence to suggest that the adult lung may, at least in part, regain its growth potential under certain conditions (5, 32). Developing research in tissue engineering and regeneration

may some day accomplish the assembly of functional lung tissue *ex vivo*, but for the mean time, facilitation of compensatory lung growth in the residual lung may be a more attainable goal to improve residual lung function after resection.

The combination of dexamethasone (10 nM), 8-bromo-3'-5'-cyclic adenosine monophosphate (cAMP) (0.1 mM), and isobutylmethylxanthine (0.1 mM), referred to as DCI, has been reported to optimally induce cell differentiation in fetal lung explants and fetal lung cells (2, 8), as well as to maintain differentiation in already differentiated type II epithelial cells (3). The effects of DCI seem to be derived from the combination of dexamethasone and elevation of cAMP, but the exact mechanisms remain unclear.

DCI administration is known to modulate the expression levels of many genes in pulmonary epithelial cells. These include keratinocyte growth factor receptor and estrogen receptor (15), which have both been reported to be involved in the facilitation of lung growth in response to lung resection or various forms of lung injury. Recently, we found that RNA silencing of thyroid transcription factor 1 (TTF-1) delayed compensatory lung growth (31). DCI is also known to induce TTF-1 in pulmonary epithelial cells (15). From these findings, we hypothesized that DCI administration may facilitate compensatory lung growth. In the present study, using a mouse postpneumectomy lung growth model, we observed the effects of DCI administration through the airway on compensatory lung growth.

MATERIALS AND METHODS

Animal experiments. Specific pathogen-free, 9-wk-old, inbred, male C57BL/6 mice, weighing ~20 g, were purchased from CLEA Japan. (Tokyo, Japan). The mice were kept in a 12:12-h light-dark cycle with free access to food and water.

The mice were randomly assigned to three experimental groups, left pneumectomy (PNX) under mechanical ventilation followed by administration of DCI in Infasurf (PNX+DCI group), left pneumectomy under mechanical ventilation followed by administration of Infasurf alone (PNX+INF group), or 9-wk-old male mice without any surgical interventions or treatment administration (NoTx group).

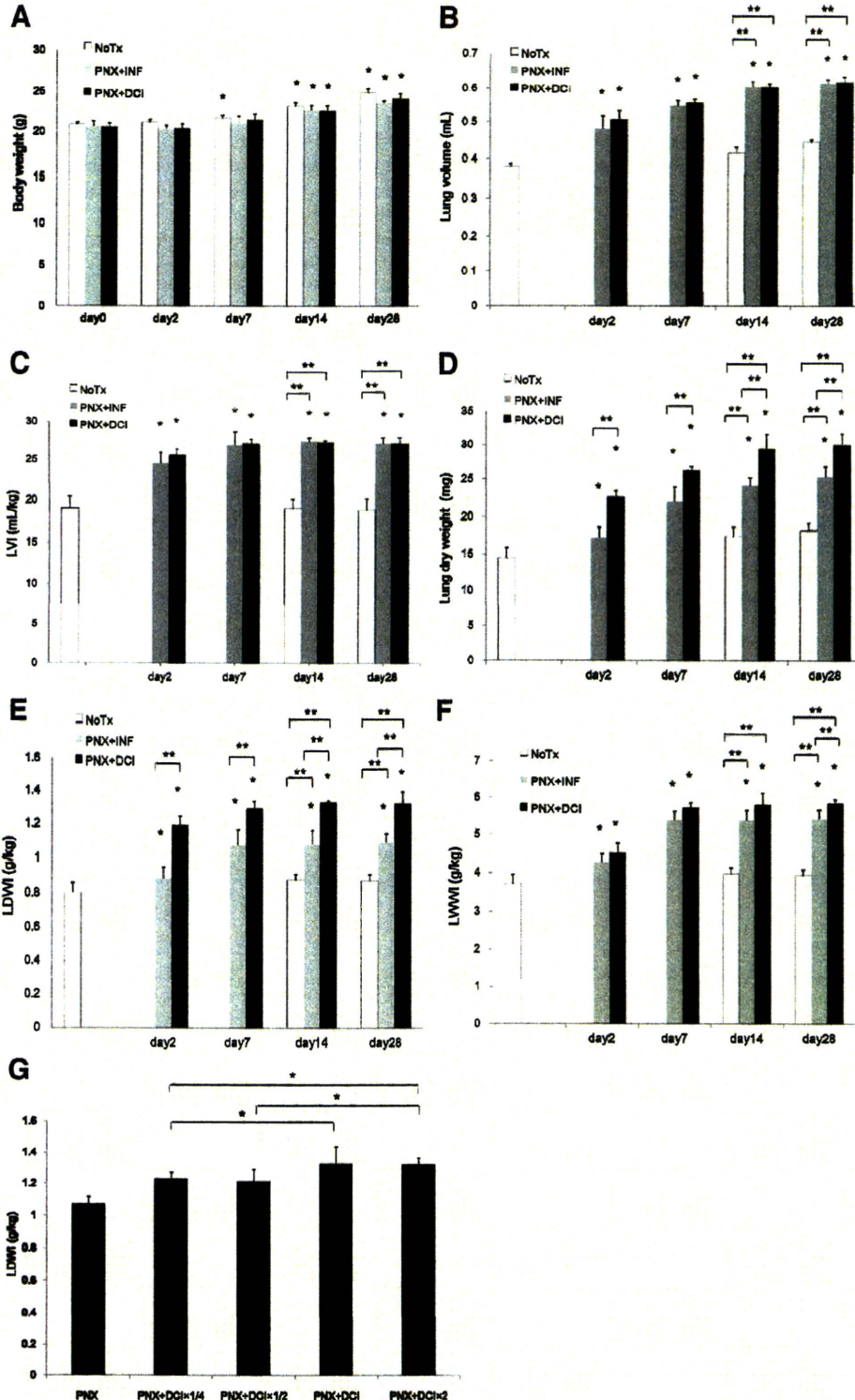
For left pneumectomy, the mice were anesthetized with 100 mg/kg of ketamine and 10 mg/kg of xylazine administered subcutaneously. They were intubated with an 18-gauge catheter and connected to a rodent ventilator, adjusted to maintain a respiratory rate of 100 breaths/min, 10 ml/kg tidal volume, 2 cmH₂O positive end-expiratory pressure, and 0.21 inspired oxygen. A 20-mm-long postero-lateral skin incision was made, followed by thoracotomy in the fifth intercostal space with dissection of the serratus anterior and latissimus dorsi muscles. Left pneumectomy was done by resecting the whole left lung from the pleural cavity. The left main bronchus with left pulmonary artery and vein were ligated at the hilum with a

Address for reprint requests and other correspondence: Y. Izumi, Division of General Thoracic Surgery, Dept. of Surgery, School of Medicine, Keio Univ., 35 Shinanomachi, Shinjuku-ku, Tokyo 160-8582, Japan (e-mail: yotarozumi@a2.keio.jp).

5–0 silk suture before removal of the lung. The tidal volume was reduced from 10 to 6 ml/kg after the lung was removed. The fifth intercostal space was closed with a single surgical suture, and the skin and muscle incisions were closed with two sutures to avoid excessive tension on the muscles. The duration of mechanical ventilation for the whole surgical

procedure was ~10 min. All mice recovered quickly after termination of mechanical ventilation and were promptly extubated.

After left pneumonectomy, DCI, a mixture of dexamethasone (500 ng/g; Sigma), 8-bromo-cAMP (5 µg/g; Santa Cruz Biotechnology, Santa Cruz, CA), and 3-isobutyl-1-methylxanthine (12.5 µg/g; Cal-



biochem, La Jolla, CA), was administered intranasally, as previously reported (18), with Infasurf (15 g/g; Ony, Amherst, New York) as a surface-active material (INF+DCI group). Infasurf alone was administered as a control (INF group). The *in vivo* dosage of DCI was extrapolated from the previously reported *in vitro* data (15), *in vivo* data (18, 36), and from our own experiences in the comparisons of *in vitro* vs. *in vivo* gene silencing using siRNAs. Administration into the nasal orifices was done using a microliter pipetter as a total of ~25 μ l. The administration was done ~30 min after extubation in both groups, at which time the mice had sufficiently recovered breathing but were still immobilized. Nine-week-old male mice without any surgical interventions or treatment were also evaluated as NoTx group.

The mice were weighed and were observed daily for any signs of distress or changes in behavior. The mice were killed at indicated time points by injection of 100 mg/kg of ketamine and 10 mg/kg of xylazine, followed by exsanguination from the inferior vena cava. The right lung was resected at designated time points for histology or Western blot analysis, as described previously.

All experimental protocols were reviewed by the Committee on the Ethics of Animal Experiments at the School of Medicine, Keio University, and were carried out in accordance with Guidelines for Animal Experiments, issued by the School of Medicine, Keio University Experimental Animal Center.

Morphological analyses. For morphological analyses, the right lung was inflated with intratracheal instillation of 10% buffered formalin at a pressure of 20 cmH₂O. The trachea was tied under pressure, and the lung was fixed in the chest cavity for 48 h before removal. Total right lung volume was measured from the fixed specimen by volume displacement, as described by Scherle (29) as the lung volume (LV) and was also normalized to the body weight as lung volume index (LVI). The lung tissue was then embedded in paraffin and cut sagittally in 4- μ m sections. Hematoxylin-and-eosin staining was done for histological analyses. Alveolus area was traced and calculated using Image J. Morphologically, alveoli were identified as polyhedral, cup, or wedged-shaped terminal air spaces with discrete septae, whereas terminal, somewhat elongated air spaces from which alveoli emerged, were considered as alveolar ducts (9). The alveolar surface area per unit of lung volume (SVw) was measured, as previously described by Weibel (34) and Kawakami et al. (10). Briefly, a standard line of the same length (LT) was drawn on the field, and intersections with this line were counted (Iw). SVw was calculated as SVw = 2 Iw/LT. For each analysis, one section was randomly selected per animal, and 5,200-fold magnification fields were randomly selected per section. The slides were coded and masked for identity and were examined by Y. Takahashi and E. Ikeda.

Lung weight measurements. The lung weight was measured as a gross assessment of compensatory lung growth. The resected lungs were lightly patted dry, weighed, and normalized to the body weight as the lung wet weight index (LWWI). The resected lungs were also completely dried in a vacuum drying oven (DP22; Yamato Scientific, Tokyo, Japan) at 95°C, and at -270 cmH₂O for 48 h, and then were weighed as the lung dry weight (LDW) and was also normalized to the body weight as the lung dry weight index (LDWI).

Transpulmonary pressure measurements. Transpulmonary pressures were measured in separate groups of animals by modifying previously reported methods (14, 30). The animals were killed by injection of 100 mg/kg of ketamine and 10 mg/kg of xylazine, followed by exsanguination from the inferior vena cava, 14 days after interventions in PNX (*n* = 5), PNX+INF (*n* = 5), and PNX+DCI (*n* = 5) groups. The animal was intubated, and the intubation tube was connected to an injection syringe and a water manometer (Innomedics Medical Instruments, Tokyo, Japan) by a three-way stopcock. The diaphragm was observed through the laparotomy. The lung was assumed to be at functional residual capacity after death, which was in agreement with the position of the diaphragm observed through the laparotomy. The lung was inflated by air at 0.1-ml increments, up to maximum inspiration observed by the position of the diaphragm, and then it was derecruited by deflation at 0.1-ml increments. Lung deflation was observed through the diaphragm. Intratracheal pressure during deflation was measured by the water manometer as the transpulmonary pressure. Static compliance was calculated as the slope of the curve from 0 to 5 cmH₂O of transpulmonary pressure.

Western blot analysis for TTF-1. For TTF-1 Western blot analysis, the right lung was resected at respective time points, blotted dry, immediately snap frozen in liquid nitrogen, and stored in -80°C. Western blot analysis for TTF-1 protein was performed according to a standard protocol. Briefly, lung tissue was lysed with a denaturing RIPA buffer (Sigma, Stockholm, Sweden), and the lysate was centrifuged at 14,000 rpm for 15 min at 4°C, and the supernatant was mixed with Laemmli buffer and applied to SDS-PAGE gels. The proteins were separated by 12.5% SDS-PAGE under reducing conditions and then transferred to PVDF membrane for 90 min at 90 V using HorizBlot system (ATTO, Tokyo, Japan). After blocking nonspecific reactions with Block Ace (Dainippon Pharmaceutical, Osaka, Japan), the primary antibody for TTF-1 (H-190; Santa Cruz Biotechnology, Santa Cruz, CA) and the antibody for β -actin (Abcam, Cambridge, UK) were incubated with the blot overnight at 4°C. The secondary anti-rabbit IgG: ECL anti-rabbit IgG horseradish peroxidase linked with whole antibody (GE Healthcare, Little Chalfont, Buckinghamshire, UK) was incubated with the blots for 1 h at room temperature.

Fig. 1. Changes in lung volume index and lung weight index after pneumonectomy and administration of a combination of dexamethasone, 8-bromo-3'-5'-cyclic adenosine monophosphate, and isobutylmethylxanthine (DCI). A: overall, the body weight of the mice was increased over time reflecting growth. The body weight of the mice was reduced in the left pneumonectomy (PNX)+DCI (*n* = 5) and PNX+ administration of Infasurf alone (INF; *n* = 5) groups compared with the NoTx (*n* = 5) group beyond day 2, but statistical significance was not reached. The body weight of the mice did not differ significantly between the PNX+DCI group and the PNX+INF group throughout the experiment period. **P* < 0.05 vs. day 0 of the same group. B: residual right lung volume index (LV) was increased significantly beyond day 2 in both the PNX+DCI (*n* = 5 at each time point) group and the PNX+INF (*n* = 5 at each time point) group compared with the NoTx (*n* = 5 at each time point) group. Within the PNX+DCI group and the PNX+INF group, there were no statistically different increases beyond day 2. There was no statistical difference in LV between the PNX+DCI group and the PNX+INF group. **P* < 0.05 vs. NoTx group. C: residual right lung volume index (LVI) was increased significantly beyond day 2 in both the PNX+DCI (*n* = 5 at each time point) group and the PNX+INF (*n* = 5 at each time point) group compared with the NoTx (*n* = 5 at each time point) group. Within the PNX+DCI group and the PNX+INF group, there were no statistically different increases beyond day 2. There was no statistical difference in LVI between the PNX+DCI group and the PNX+INF group. **P* < 0.05 vs. NoTx group. D: residual right lung dry weight (LDW) was significantly increased in the PNX+DCI (*n* = 5 at each time point) group compared with the PNX+INF (*n* = 5 at each time point) group and the NoTx (*n* = 5 at each time point) group beyond day 2. **P* < 0.05 vs. NoTx group, ***P* < 0.05 between the indicated groups. E: residual right lung dry weight index (LDWI) was significantly increased in the PNX+DCI (*n* = 5 at each time point) group compared with the PNX+INF (*n* = 5 at each time point) group and the no treatment (NoTx; *n* = 5 at each time point) group beyond day 2. **P* < 0.05 vs. NoTx group, ***P* < 0.05 between the indicated groups. F: residual right lung wet weight index (LWWI) tended to be higher in the PNX+DCI (*n* = 5) group compared with the PNX+INF (*n* = 5 at each time point) group and the NoTx (*n* = 5 at each time point) group beyond day 2. **P* < 0.05 vs. NoTx group, ***P* < 0.05 between the indicated groups. G: LDWI at day 14 was compared between different dosages of DCI (*n* = 5 in each group). One quarter, one half, and twofold amounts were administered. The twofold dose did not induce further increase in LDWI, while one-half or one-quarter dosage attenuated the increase in LDWI. Hence, the dosage used in this study was considered to be most suitable within the dosages evaluated. **P* < 0.05 between the indicated groups.

Bands were detected by enhanced chemiluminescence using ECL Western blotting detection reagents (Amersham Bioscience, Piscataway, NJ). Band densitometry was quantified using Image J (National Institutes of Health, Bethesda, MD). Values were normalized to β -actin.

RNA silencing of TTF-1. TTF-1 silencing small inhibitory RNA oligonucleotides, si#2 and si#4 (Invitrogen, Carlsbad, CA) were selected and administered as previously described (29). This method of administration has been shown to effectively reduce TTF-1 expression level in the lung after pneumonectomy. Sequences of si#2 and si#4 were (5'-UUGAAACGUCGUCGAGCUCGUACA-3') and (5'-GCUACAA-GAUGAAGCGCCGCUAA-3'), respectively. Thirty-five milligrams per kilogram of each inhibitory RNA was coadministered intranasally with DCI.

Exercise tests. Exercise function was tested using wheel-running tests (wheel circumference 75 cm) as an indirect index of lung function after pneumonectomy (23). Before each test, the mice were adapted to the wheel by ~200 rounds of voluntary wheel running. First, as an index of forced exercise, the mouse was placed on the wheel, and the wheel was manually spun at one round per second. This was continued until the mouse was unable to cope and was spun with the wheel, and the number of rounds was recorded. This was repeated 3 times with 5-min breaks in between, and was averaged. Next, after a 30-min break, as an index of semivoluntary exercise, the mouse was placed on the wheel, and the number of rounds spun in 5 min was recorded. The mouse was facilitated to run by touching on the tail if it stood still for longer than 5 s. Measurements were taken before pneumonectomy (*day 0*), and on *day 2*, *day 7*, and *day 14* after pneumonectomy and respective material administration. The NoTx group did not receive any treatment or surgery.

Statistical analysis. Data are expressed as means \pm SD. Comparisons between groups were done using Mann-Whitney *U*-test (StatView; Abacus, Berkeley, CA). Body weight and exercise tests were compared within groups using paired *t*-test (StatView; Abacus). Other comparisons within groups were done using Mann-Whitney *U*-test since the animals were killed for respective time point measurements. *P* values less than 0.05 were considered to be statistically significant.

RESULTS

Lung volume and lung weight measurements. The body weight of the mice tended to increase within each group during the period of the experiment reflecting animal growth. It was reduced in the PNx+DCI ($n = 5$) and PNx+INF ($n = 5$) groups compared with the NoTx ($n = 5$) group beyond *day 2*, but statistical significance was not reached. The body weight of the mice did not differ significantly between the PNx+DCI group and the PNx+INF group throughout the experiment period (Fig. 1A). Therefore, it was considered feasible to compare weight-based indices between these groups.

The residual right LV and LVI were increased significantly beyond *day 2* in both the PNx+DCI ($n = 5$ at each time point) group and the PNx+INF ($n = 5$ at each time point) group compared with the NoTx ($n = 5$ at each time point) group. Within the PNx+DCI group and the PNx+INF group, there were no statistically different increases beyond *day 2*. There was no statistical difference between the PNx+DCI group and the PNx+INF group (Fig. 1, B and C).

In contrast to the changes in LV and LVI, the residual right LDW and LDWI was significantly increased in the PNx+DCI ($n = 5$ at each time point) group compared with the PNx+INF ($n = 5$ at each time point) group and the NoTx ($n = 5$ at each time point) group beyond *day 2* (Fig. 1, D and E). The magnitude of increase in LDWI in the PNx+INF group was similar to the previous data on left pneumonectomy alone (31). The LWI also showed a similar tendency, although the

difference between the PNx+DCI ($n = 5$ at each time point) group and the PNx+INF ($n = 5$ at each time point) reached statistical significance only on *day 28* (Fig. 1F).

The effect of DCI dosage on LDWI was also evaluated. The LDWI at *day 14* was compared between different dosages ($n = 5$ in each group) (Fig. 1G). The twofold dose did not induce further increase in LDWI, while one-half or one-quarter dosage attenuated the increase in LDWI. Hence, the dosage used in this study was considered to be most suitable within the dosages evaluated, at least in this particular model. DCI administration to mice without pneumonectomy did not induce any changes in LDWI.

Western blot analysis. Western blot analysis showed that TTF-1 expression in the residual right lung at *day 2* was significantly increased in the PNx+DCI group compared with pneumonectomy only (PNx group), the PNx+INF group or the NoTx group (Fig. 2A). We also concomitantly administered TTF-1 inhibitory RNAs (TTF-1 siRNAs) with DCI after pneumonectomy. The increase in LDWI by DCI administration was not affected by coadministration of TTF-1 siRNAs at *day 2* ($n = 5$ in each group) but was significantly suppressed at *day 7* by TTF-1 siRNAs ($n = 5$ in each group) (Fig. 2B).

Morphological analyses. On histology, the alveoli appeared to be smaller in the PNx+DCI group compared with the PNx+INF group or the NoTx group at *day 7* (Fig. 3A). Morphological analyses showed that the number of alveoli per field of view was significantly increased in the PNx+DCI group compared with the PNx+INF group and the NoTx group throughout the experiment (Fig. 3B). The average traced area of a single alveolus on histology was significantly decreased in the PNx+DCI group compared with the PNx+INF group and the NoTx group beyond 7 days (Fig. 3C). The traced total alveolar area per field was significantly increased in the PNx+DCI group compared with the PNx+INF group and the NoTx group beyond 2 days (Fig. 3D). The calculated surface area of the alveoli per volume of lung was also significantly increased in the PNx+DCI group compared with the PNx+INF group and the NoTx group at *day 28* (Fig. 3E).

Transpulmonary pressure measurements. The changes in transpulmonary pressure at *day 14* was not significantly different between PNx ($n = 5$), PNx+INF ($n = 5$), and the PNx+DCI ($n = 5$) groups (Fig. 4). The calculated static compliance was also not statistically different between groups [PNx, PNx+INF, and PNx+DCI groups, 186.8 ± 8.5 , 190.8 ± 6.8 , and 192.4 ± 5.0 , 10^{-3} ml/cm H₂O, respectively ($P > 0.05$)].

Exercise tests. General appearance, movement, and feeding behavior were similar between the PNx+DCI group and the PNx+INF group throughout the experiment period. Forced wheel running ($n = 4$ in each group) at *day 2* was significantly reduced in both groups compared with *day 0*. Recovery was seen beyond *day 7* in the PNx+DCI group but not in the PNx+INF group (Fig. 5A). Semivoluntary wheel running at *day 2* tended to be reduced in both PNx+DCI and PNx+INF groups compared with *day 0*. Recovery was seen at *day 7* in both groups without statistically significant differences. At *day 14*, the PNx+DCI group and the NoTx group showed significantly increased semivoluntary wheel running compared with their respective *day 0* values, presumably reflecting adaptation to wheel running, but the PNx+INF group remained at a similar level as *day 7*. The difference at *day 14* was significant between the PNx+DCI group and the PNx+INF group (Fig. 5B).

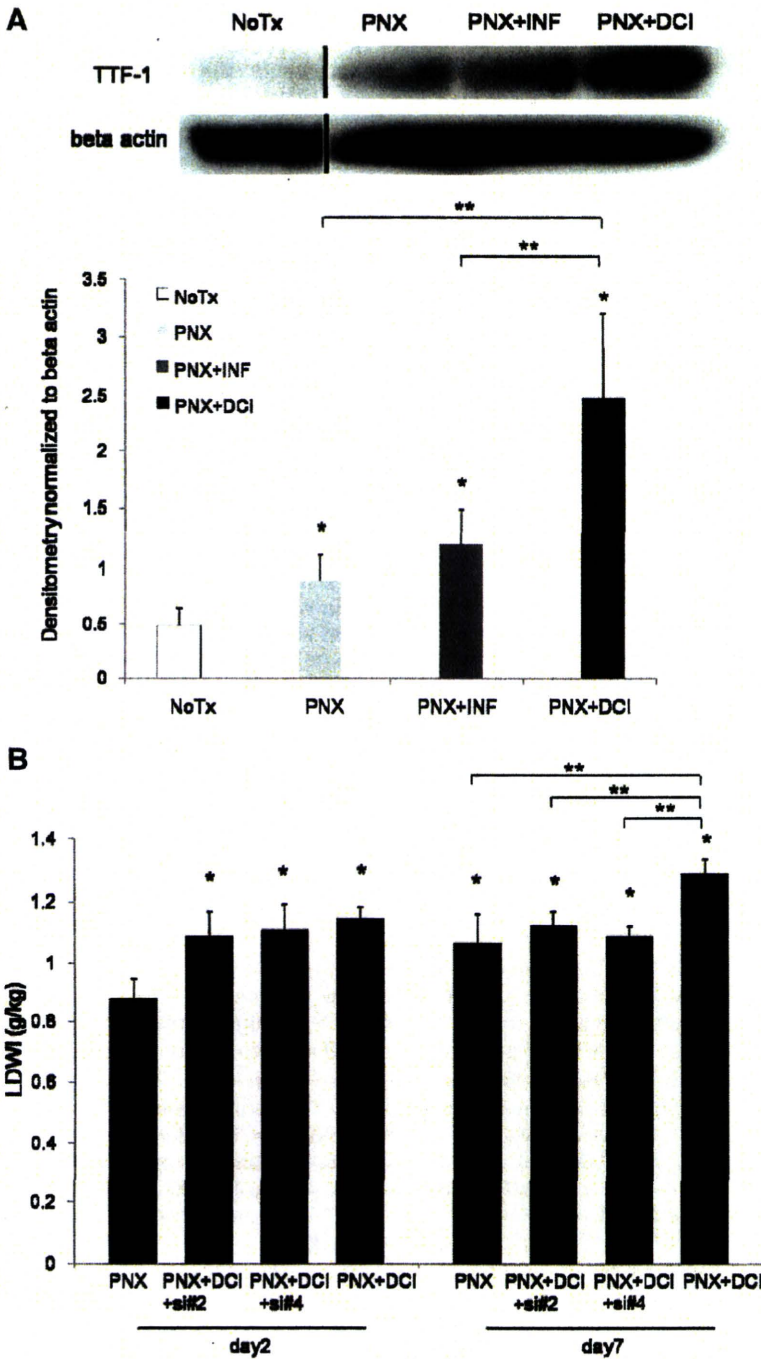


Fig. 2. A: Western blot analysis showed that thyroid transcription factor 1 (TTF-1) expression in the residual right lung at day 2 was significantly increased in the PNx+DCI group compared with PNx only (PNx group), PNx+INF group, or the NoTx group. The NoTx group and the respective β -actin is from a different gel. Band densitometry was quantified using Image J. Values were normalized to β -actin. * $P < 0.05$ vs. NoTx group, ** $P < 0.05$ between the indicated groups. B: increase in right LDWI by DCI administration after left pneumonectomy was not affected by coadministration of TTF-1 inhibitory RNAs (TTF-1 siRNAs), si#2, and si#4, at day 2 ($n = 5$ in each group) but was significantly suppressed at day 7 by both sequences of TTF-1 siRNAs ($n = 5$ in each group). * $P < 0.05$ vs. NoTx group, ** $P < 0.05$ between the indicated groups.

DISCUSSION

In the present study, compensatory lung growth was modestly but significantly facilitated by airway administration of DCI, as indicated by the increase in LDW and LDWI. Morphological analyses suggested that DCI administration increased the number alveoli, made each of them smaller, and produced a net increase in the total alveolar area per field and the calculated surface area of the alveoli per volume of lung. Similar findings have been reported with retinoic acid (4, 21, 22) and estrogen (19, 20). These findings may merely represent

an imbalance between septation and septal cell proliferation, but it is also possible that DCI administration reduced lung elasticity. To this end, at least morphologically, there were no apparent indications of atelectasis, pleural thickening, septal thickening, or inflammation in the PNx+DCI group. There was also no significant difference between the PNx+INF group and the PNx+DCI group in transpulmonary pressure at day 14. Therefore, the spatial constraint due to the predetermined volume of the chest cavity, which presumably resulted in the lack of significant increase in LVI, may

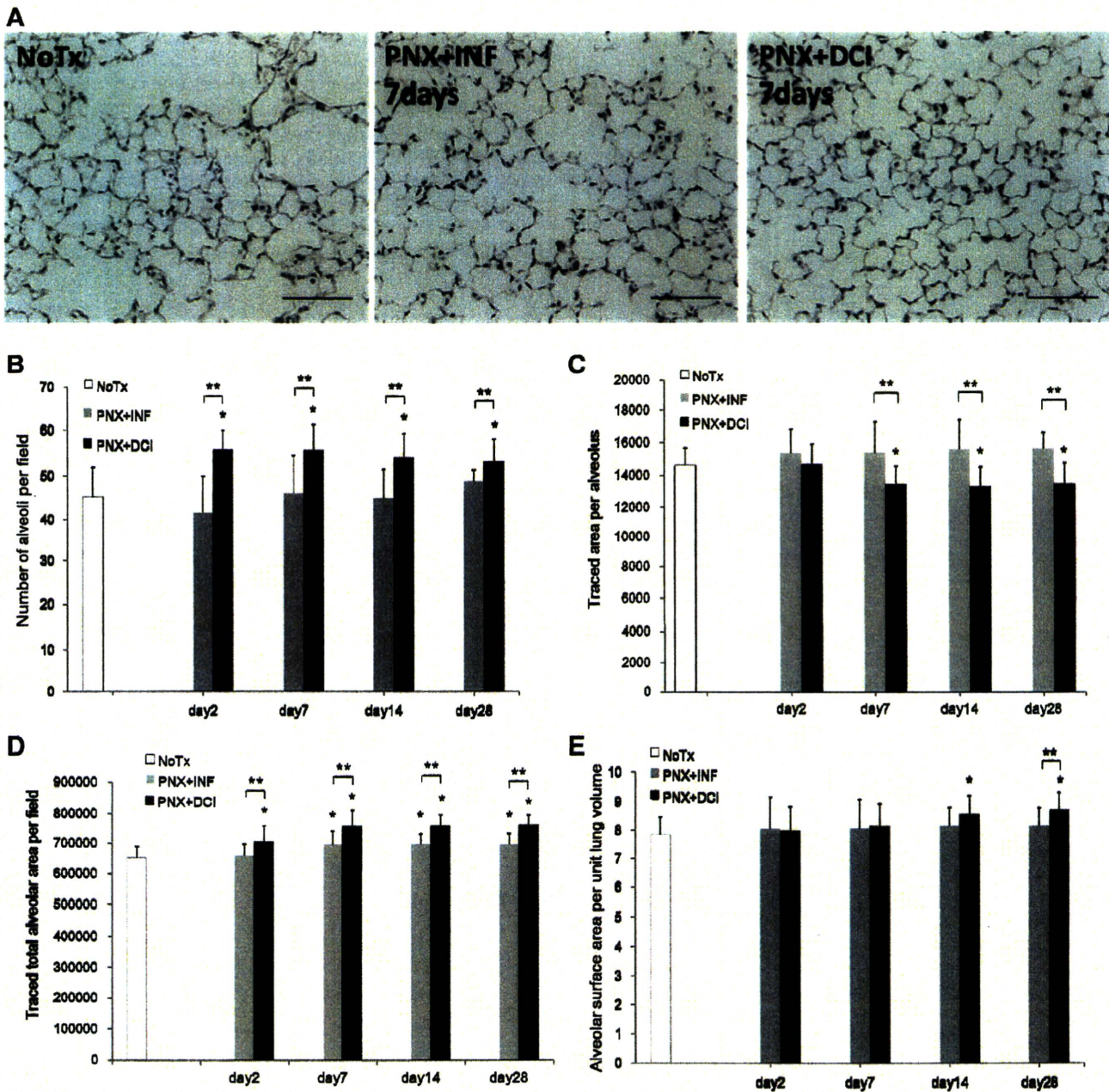


Fig. 3. Morphological findings. *A*: on morphology at *day 7*, the alveoli appeared to be smaller in the PNX+DCI group compared with the PNX+INF group or the NoTx group. Hematoxylin-and-eosin staining, scale bar 100 μm . *B*: on morphological analysis, the number of alveoli per field of view was significantly increased in the PNX+DCI ($n = 5$; 25 fields for each time point) group compared with the PNX+INF ($n = 5$; 25 fields for each time point) group and the NoTx ($n = 5$; 25 fields for each time point) group throughout the experiment. *C*: average traced area of a single alveolus on morphology was significantly decreased in the PNX+DCI ($n = 5$; 25 fields for each time point) group compared with the PNX+INF ($n = 5$; 25 fields for each time point) group, and the NoTx ($n = 5$; 25 fields for each time point) group beyond 7 days. *D*: average total alveolar area per field on morphology was significantly increased in the PNX+DCI ($n = 5$; 25 fields for each time point) group compared with the PNX+INF ($n = 5$; 25 fields for each time point) group and the NoTx ($n = 5$; 25 fields for each time point) group beyond 2 days. *E*: calculated surface area of the alveoli per volume of lung was significantly increased in the PNX+DCI ($n = 5$; 25 fields for each time point) group compared with the PNX+INF ($n = 5$; 25 fields for each time point) group and the NoTx ($n = 5$; 25 fields for each time point) group beyond *day 14*. * $P < 0.05$ vs. NoTx group, ** $P < 0.05$ between the indicated groups.

at least, in part, be the reason for these findings. Since morphological analyses were carried out in fixed specimens, it is also not possible to completely rule out the possibility that the fixation-induced shrinkage may have been different among groups. Further studies looking into the extracellular

matrix components may resolve some of these issues, but collectively, the data suggest that the increase in LDWI was primarily due to the increase in the number of alveoli. If so, increased number of small alveoli may have actually augmented lung function within a fixed lung volume (19). To

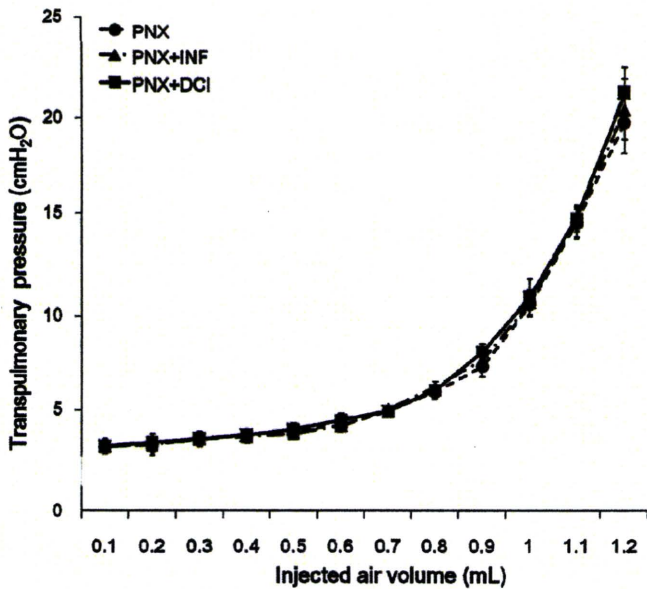


Fig. 4. Transpulmonary pressure measurements were made using a water manometer at increments of 0.1 ml. The curve shape was not significantly different between the PNX group ($n = 5$), PNX+INF group ($n = 5$) and the PNX+DCI group ($n = 5$).

this end, exercise capability, particularly forced exercise, which has been reported to reflect lung function (23), was better sustained in the PNX+DCI group compared with the PNX+INF group, although it is possible that factors other than lung function may also have contributed to this difference. The results of the semivoluntary wheel-running test, at least in part, rules out the possibility that DCI administration caused alterations in spontaneous activity of mice, which may have influenced the results of the exercise tests. To this end, more detailed specific lung function tests are required.

Glucocorticoids potentially induce developmental lung growth (1) but is reported to have no apparent effect on compensatory lung growth by systemic administration (25). Induction of cAMP has been shown to facilitate fetal lung maturation (2), and in combination with dexamethasone, this facilitation has been shown to be synergistic (8). The exact mechanism of this synergy remains unclear, and furthermore, the effects of glucocorticoids on developmental and postnatal lung growth seem to be context dependent. Developmental, postnatal, and postpneumonectomy compensatory lung growth may be regulated through different pathways although not mutually exclusive. Hence, it is possible that glucocorticoids and cAMP, individually and in combination, may act differently on each of the lung growth processes. Caution in the use of dexamethasone may be required since prolonged systemic administration of glucocorticoids, particularly at high doses, are reported to be detrimental to postnatal lung growth (6, 26). Although the combined effects of the components of DCI may be substantially different from the effects of glucocorticoids alone, it is nevertheless encouraging that in the present study, the effect of a single administration of DCI was sustained for at least 28 days. Although we have not done any pharmacokinetic studies, it is unlikely that the effect of DCI per se was sustained throughout this period, suggesting that facilitation

of initial stimuli for compensatory lung growth is important rather than its maintenance. Therefore, prolonged administration may not be necessary. Furthermore, administration of DCI without pneumonectomy did not demonstrate any overt effects (data not shown), suggesting that DCI only augments compensatory lung growth. To this end, the optimal timing of DCI administration in relation to pneumonectomy, along with the potential duration of action of DCI is considered to be important and requires further study.

In the present study, we used INF as a vehicle since it is in clinical use as a surfactant supplement and is experimentally

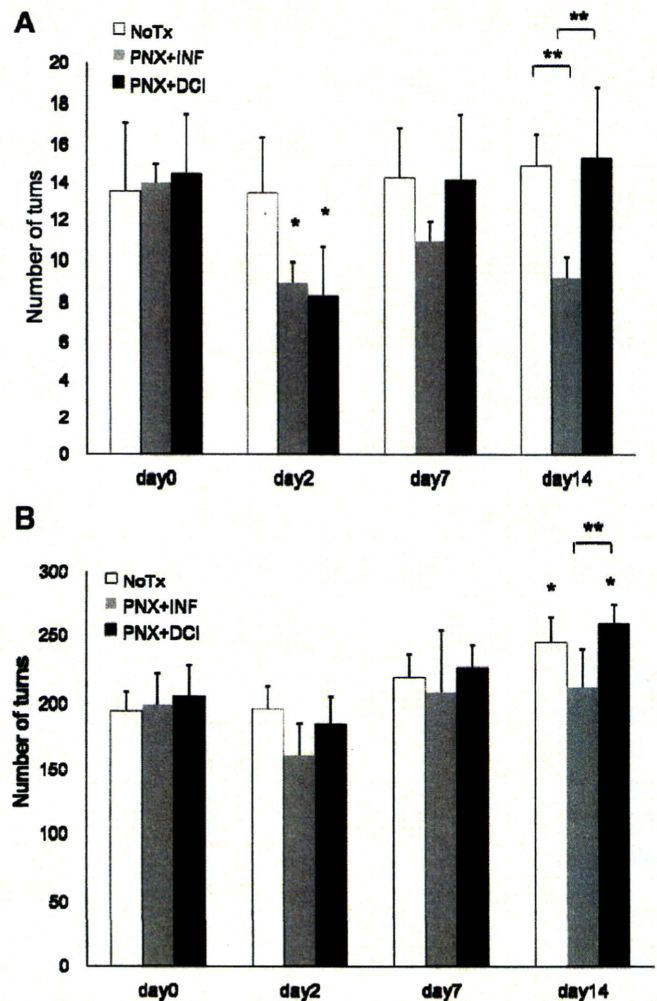


Fig. 5. Exercise tests as indirect indices of lung function. A: forced wheel running at day 0, prior to pneumonectomy, did not differ significantly between groups ($n = 4$ in each group). Forced wheel running at day 2 was significantly reduced in both PNX+DCI and PNX+INF groups compared with the respective values at day 0. Recovery was seen beyond day 7 in the PNX+DCI group but not in the PNX+INF group. * $P < 0.05$ vs. respective day 0 values, ** $P < 0.05$ between the indicated groups. B: semivoluntary wheel running at day 2 ($n = 4$ in each group) tended to be reduced in both PNX+DCI and PNX+INF groups compared with day 0. Recovery was seen at day 7 in both groups without statistically significant differences. At day 14, the PNX+DCI group and the NoTx group were significantly increased compared with their respective day 0 values, presumably reflecting adaptation to wheel running, but the PNX+INF group remained at a similar level as day 7. The difference at day 14 was significant between the PNX+DCI group and the PNX+INF group. * $P < 0.05$ vs. respective day 0 and day 2 values, ** $P < 0.05$ between the indicated groups.

reported to facilitate the movement of coadministered materials into the airway from the nasal orifice (18). Other surface-active materials may also be effective. The delivery of inhaled all-trans-retinoic acid has been previously reported in detail (17), showing that airway administration is expected to be most efficient in delivering materials to the lung. However, it is possible that systemic concentration of DCI was also significantly elevated in this particular study, since at least a fraction of administered DCI was expected to be absorbed from the nasal mucosa, even with INF. Further delivery and pharmacokinetic studies are necessary to address these issues.

Growth factors such as epidermal growth factor (11), hepatocyte growth factor (27), vascular endothelial growth factor (28), and keratinocyte growth factor (13), and a form of vitamin, retinoic acid (12), have been reported to facilitate compensatory lung growth. Our previous study suggested the importance of TTF-1 in compensatory lung growth (31). The results of the present study indicate that DCI administration augments the induction of TTF-1 after pneumonectomy in the lung in vivo. Although the effect of DCI is likely to be multifaceted, the induction of TTF-1 may, at least in part, be involved in the effects of DCI on facilitating compensatory lung growth, since concomitant administration of TTF-1 siRNAs suppressed the effects of DCI on day 7, although this effect was not apparent on day 2. It is possible that the induction of TTF-1 by DCI may have peaked earlier than day 2. Administration of siRNAs at earlier time points, namely before pneumonectomy, may, to some extent, clarify this issue. Further studies to specify the types of alveolar septal cells affected by DCI are also necessary.

To our knowledge, this is the first report of a material administered through the airway, which facilitates compensatory lung growth. Airway administration would be an ideal route of application in the clinic for materials that are expected to function in the lung. Furthermore, DCI may have advantages over the administration of growth factors in that it is a combination of materials that are clinically accessible and that it is also expected to be more acceptable in terms of cost. Although still preliminary, DCI with further modifications may provide a therapeutic treatment to potentially augment residual lung function after resection.

ACKNOWLEDGMENTS

The authors thank Kei Tsujioka, Division of General Thoracic Surgery, School of Medicine, Keio University, for her expertise in animal experiments.

GRANTS

This work was supported, in part, by grant in aid from the Ministry of Education, Culture, Sports, Science, and Technology-Japan, and the School of Medicine, Keio University fund for the promotion of science.

DISCLOSURES

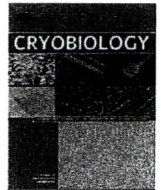
No conflicts of interest, financial or otherwise are declared by the authors.

REFERENCES

- Ad Hoc Statement Committee, American Thoracic Society. Mechanisms and limits of induced postnatal lung growth. *Am J Respir Crit Care Med* 170: 319–343, 2004.
- Ballard PL, Gonzales LW, Williams MC, Roberts JM, Jacobs MM. Differentiation of type II cells during explant culture of human fetal lung is accelerated by endogenous prostanoids and adenosine 3',5'-monophosphate. *Endocrinology* 128: 2916–2924, 1991.
- Bates SR, Gonzales LW, Tao JQ, Rueckert P, Ballard PL, Fisher AB. Recovery of rat type II cell surfactant components during primary cell culture. *Am J Physiol Lung Cell Mol Physiol* 282: L267–L276, 2002.
- Belloni PN, Garvin L, Mao CP, Bailey-Healy I, Leaffer D. Effects of all-trans-retinoic acid in promoting alveolar repair. *Chest* 117: 235S–241S, 2000.
- Binns OA, DeLima NF, Buchanan SA, Lopes MB, Cope JT, Marek CA, King Laubach VE RC, Tribble CG, Kron IL. Mature pulmonary lobar transplants grow in an immature environment. *J Thorac Cardiovasc Surg* 114: 186–194, 1997.
- Fayon M, Jouvencel P, Carles D, Choukroun ML, Marthan R. Differential effect of dexamethasone and hydrocortisone on alveolar growth in rat pups. *Pediatr Pulmonol* 33: 443–448, 2002.
- Fehrenbach H, Voswinkel R, Michl V, Mehling T, Fehrenbach A, Seeger W, Nyengaard JR. Neoalveolarisation contributes to compensatory lung growth following pneumonectomy in mice. *Eur Respir J* 31: 515–522, 2008.
- Gonzales LW, Guttentag SH, Wade KC, Postle AD, Ballard PL. Differentiation of human pulmonary type II cells in vitro by glucocorticoid plus cAMP. *Am J Physiol Lung Cell Mol Physiol* 283: L940–L951, 2002.
- Inselman LS, Padilla-Burgos LB, Teichberg S, Spencer H. Alveolar enlargement in obesity-induced hyperplastic lung growth. *J Appl Physiol* 65: 2291–2296, 1988.
- Kawakami M, Paul JL, Thurlbeck WM. The effect of age on lung structure in male BALB/cNnia inbred mice. *Am J Anat* 170: 1–21, 1984.
- Kaza AK, Laubach VE, Kern JA, Long SM, Fiser SM, Tepper JA, Nguyen RP, Shockey KS, Tribble CG, Kron IL. Epidermal growth factor augments postpneumonectomy lung growth. *J Thorac Cardiovasc Surg* 120: 916–921, 2000.
- Kaza AK, Kron IL, Kern JA, Long SM, Fiser SM, Nguyen RP, Tribble CG, Laubach VE. Retinoic acid enhances lung growth after pneumonectomy. *Ann Thorac Surg* 71: 1645–1650, 2001.
- Kaza AK, Kron IL, Leuwerke SM, Tribble CG, Laubach VE. Keratinocyte growth factor enhances post-pneumonectomy lung growth by alveolar proliferation. *Circulation* 106: I120–I124, 2002.
- Kida K. Lack of recovery of lung structure after the administration of beta-amino-propionitrile in the postnatal period. *Am Rev Respir Dis* 122: 467–475, 2002.
- Kolla V, Gonzales LW, Gonzales J, Wang P, Angampalli S, Feinstein SI, Ballard PL. Thyroid transcription factor in differentiating type II cells: regulation, isoforms, and target genes. *Am J Respir Cell Mol Biol* 36: 213–225, 2007.
- Laros CD, Westermann CJ. Dilatation, compensatory growth, or both after pneumonectomy during childhood and adolescence. A thirty-year follow-up study. *J Thorac Cardiovasc Surg* 93: 570–576, 1987.
- March TH, Cossey PY, Esparza DC, Dix KJ, McDonald JD, Bowen LE. Inhalation administration of all-trans-retinoic acid for treatment of elastase-induced pulmonary emphysema in Fischer 344 rats. *Exp Lung Res* 30: 383–404, 2004.
- Massaro D, Massaro GD, Clerch LB. Noninvasive delivery of small inhibitory RNA and other reagents to pulmonary alveoli in mice. *Am J Physiol Lung Cell Mol Physiol* 287: L1066–L1070, 2004.
- Massaro GD, Mortola JP, Massaro D. Sexual dimorphism in the architecture of the lung's gas-exchange region. *Proc Natl Acad Sci USA* 92: 1105–1107, 1995.
- Massaro GD, Mortola JP, Massaro D. Estrogen modulates the dimensions of the lung's gas-exchange surface area and alveoli in female rats. *Am J Physiol Lung Cell Mol Physiol* 270: L110–L114, 1996.
- Massaro GD, Massaro D. Postnatal treatment with retinoic acid increases the number of pulmonary alveoli in rats. *Am J Physiol Lung Cell Mol Physiol* 270: L305–L310, 1996.
- Massaro GD, Massaro D. Retinoic acid treatment partially rescues failed septation in rats and in mice. *Am J Physiol Lung Cell Mol Physiol* 278: L955–L960, 2000.
- Morani A, Barros RP, Imamov O, Hulthenby K, Arner A, Warner M, Gustafsson JA. Lung dysfunction causes systemic hypoxia in estrogen receptor beta knockout (ERβ^{-/-}) mice. *Proc Natl Acad Sci USA* 103: 7165–7169, 2006.
- Nakajima C, Kijimoto C, Yokoyama Y, Miyakawa T, Tsuchiya Y, Kuroda T, Nakano M, Saeki M. Longitudinal follow-up of pulmonary function after lobectomy in childhood—factors affecting lung growth. *Pediatr Surg Int* 13: 341–345, 1988.

25. **Rannels DE, Karl HW, Bennett RA.** Control of compensatory lung growth by adrenal hormones. *Am J Physiol Endocrinol Metab* 253: E343–E348, 1987.
26. **Sahebajami H, Domino M.** Effects of postnatal dexamethasone treatment on development of alveoli in adult rats. *Exp Lung Res* 15: 961–973, 1989.
27. **Sakamaki Y, Matsumoto K, Mizuno S, Miyoshi S, Matsuda H, Nakamura T.** Hepatocyte growth factor stimulates proliferation of respiratory epithelial cells during postpneumonectomy compensatory lung growth in mice. *Am J Respir Cell Mol Biol* 26: 525–533, 2002.
28. **Sakurai MK, Lee S, Arsenault DA, Nose V, Wilson JM, Heymach JV, Puder M.** Vascular endothelial growth factor accelerates compensatory lung growth after unilateral pneumonectomy. *Am J Physiol Lung Cell Mol Physiol* 292: L742–L747, 2007.
29. **Scherle W.** A simple method for volumetry of organs in quantitative stereology. *Mikroskopie* 26: 57–60, 1970.
30. **Schultz H, Johner C, Edger G, Ziesenis A, Reitmeier P, Heyder J, Balling R.** Respiratory mechanics in mice: strain and sex specific differences. *Acta Physiol Scand* 174: 367–375, 2002.
31. **Takahashi Y, Izumi Y, Kohno M, Kimura T, Kawamura M, Okada Y, Nomori H, Ikeda E.** Thyroid transcription factor 1 influences the early phase of compensatory lung growth in adult mice. *Am J Respir Crit Care Med* 181: 1397–1406.
32. **Ueda K, Tanaka T, Hayashi M, Li TS, Tanaka N, Hamano K.** Computed tomography-defined functional lung volume after segmentectomy versus lobectomy. *Eur J Cardiothorac Surg* 37: 1433–1437, 2010.
33. **Voswinckel R, Motejl V, Fehrenbach A, Wegmann M, Mehling T, Fehrenbach H, Seeger W.** Characterisation of post-pneumonectomy lung growth in adult mice. *Eur Respir J* 24: 524–532, 2004.
34. **Weibel ER.** *Stereological Methods*. New York: Academic, 1979, p. 9–196.
35. **Weibel ER.** Biomorphometry in physiological and pathological research. *Acta Med Pol* 23: 115–125, 1982.
36. **Zhang X, Shan P, Jiang D, Noble PW, Abraham NG, Kappas A, Lee PJ.** Small interfering RNA targeting heme oxygenase-1 enhances ischemia-reperfusion-induced lung apoptosis. *J Biol Chem* 279: 10677–10684, 2004.





On freeze-thaw sequence of vital organ of assuming the cryoablation for malignant lung tumors by using cryoprobe as heat source [☆]

Seishi Nakatsuka ^a, Hideki Yashiro ^b, Masanori Inoue ^a, Sachio Kuribayashi ^a, Masafumi Kawamura ^{c,d}, Yotaro Izumi ^c, Norimasa Tsukada ^e, Yoshikane Yamauchi ^c, Kohei Hashimoto ^c, Kansei Iwata ^f, Taisuke Nagasawa ^{f,*}, Yi-Shan Lin ^f

^a Department of Diagnostic Radiology, School of Medicine, KEIO University, 35 Shinanomachi, Shinjuku-ku, Tokyo 160-8582, Japan

^b Hiratsuka City Hospital, 1-19-1 Minamihara, Hiratsuka, Kanagawa 254-0065, Japan

^c Division of General Thoracic Surgery, School of Medicine, KEIO University, 35 Shinanomachi, Shinjuku-ku, Tokyo 160-8582, Japan

^d Division of General Thoracic Surgery, School of Medicine, TEIKYO University, 2-11-1 Kaga, Itabashi-ku, Tokyo 173-0003, Japan

^e Kawasaki Municipal Hospital, Shinkawadori, Kawasaki-ku, Kawasaki, Kanagawa 210-0013, Japan

^f DgS Computer Co., Ltd., 2-27 Minamiosawa, Hachioji, Tokyo 192-0364, Japan

ARTICLE INFO

Article history:

Received 8 April 2010

Accepted 18 October 2010

Available online 29 October 2010

Keywords:

Freezing function

Freeze-thaw sequence

Isothermal curve

Cryosurgery

Cryoablation

Lung cancer

Joule–Thomson effect

Porcine lung

ABSTRACT

Regarding cryoablation for the malignant lung tumors, multiple trials of the freeze-thaw process have been made, and we considered it necessary to view and analyze the freeze-thaw process as a freeze-thaw sequence. We caused the sequence in a porcine lung *in vivo* by using an acicular, cylindrical stainless-steel probe as the heat source for the freeze-thaw sequence and cooling to $-150\text{ }^{\circ}\text{C}$ with super high-pressure argon gas by causing the Joule–Thomson effect phenomenon at the tip of the probe. In this experiment, we examined the sequence by measuring the temperature and using the isothermal curve and the freezing function. As a result, it was demonstrated that the freezing characteristics considerably differed in the first sequence and the second sequence from those of non-aerated organs such as liver and kidney. In our experiments on porcine lung, thermal properties were considered to change as the bleeding caused by the first thawing infiltrated in the lung parenchyma, and it was confirmed that the frozen area in the second cycle was dramatically enlarged as compared with the first cycle (when a similar sequence is continuously repeated, we say it as cycle). This paper provides these details.

© 2010 Elsevier Inc. All rights reserved.

The cryoablation for the malignant lung tumors is a treatment to cause local cell necrosis by a rapid freezing/thawing at the tip of the cryoprobe. Percutaneous cryoablation of lung tumors by using the Joule–Thomson effects with high-pressure argon gas and high-pressure helium gas has been safely performed under CT fluoroscopic guidance in our institute [1,2]. A cycle of the 5–10 min freezing and the thawing creates the frozen area, which was enlarged after repetition of the cycles.

There have been a large number of studies about cryoablation [3], but there are few experimental studies about the lung cryoablation [4–7]. We have made both theoretical and experimental analyses about the enlargement of the freezing surface of a normal porcine lung in order to necrose cells infallibly during cryoablation [8,9]. In this connection, we have conducted the prediction of the freezing progress in lung tumors by using a two-dimensional heat

conduction analysis with an enthalpy method and a one-dimensional heat conduction analysis with an approximation equation. The results of these two methods gave similar results. We made a theoretical prediction that there was a limit (limiting radius) to an iceball *in vivo* or a freezing limitation due to the heat balance between the cryogenic temperature of the cryoprobe as a cryogen and the heat source of the surrounding area. In the experiments, on the other hand, we conducted each trial of freezing on a porcine lung with a cryoprobe and measured the size of a frozen area. As a result, we confirmed that the theoretical calculation used in the previous paper [9] on the freezing curve reproduced the experimental values. To analyze the freezing characteristics such as the limiting radius, we defined the freezing function $f(t)$ of time t indicating the radius of freezing surface of the iceball as follows:

$$f(t) = a \exp(bt) + c (a, b < 0, c > 0). \quad (1)$$

Then, we fitted free parameters, a , b and c , to experimental data with the least-square method. Although freezing function is a non-linear function, when the time is infinite, its first term becomes zero and freezing function converges to the intercept c which is equivalent to the value of the limiting radius of the iceball. As a

[☆] Statement of funding: This work was supported by Grant-in-Aid for Scientific Research (21591823) of the Japanese Ministry of Education, Culture, Sports, Science and Technology (MK).

* Corresponding author.

E-mail address: nagasawa@dgs.co.jp (T. Nagasawa).

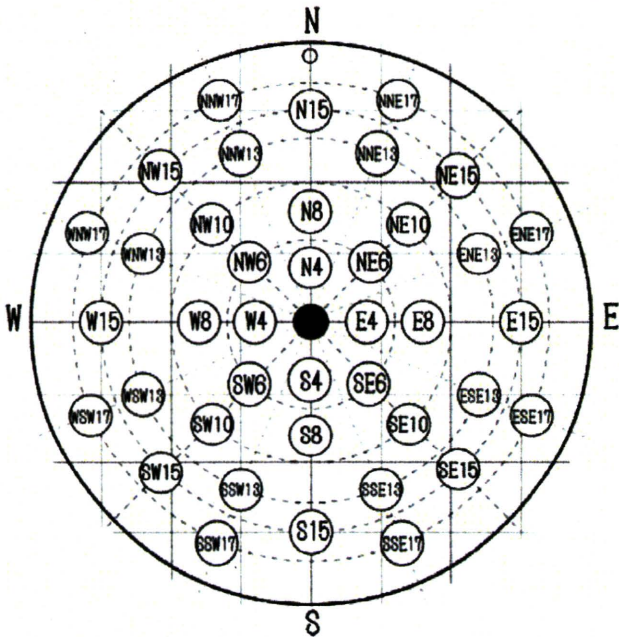


Fig. 1. Positions of the cryoprobe (center) and the thermocouples. N, E, S, and W stand for North, East, South and West, respectively and the numbers indicate the distance (mm) from the center, where the cryoprobe is positioned.

result of the analysis using this freezing function, it was found that the iceball reaches the equilibrium state in approximately 300 s at single freezing of the posterior lobe of the porcine lung and the measured limiting radius was about 10 mm. In order to verify the effectiveness of multiple cycles in cryoablation for malignant lung tumors, we conducted triple freeze-thaw cycle using the cryoprobe; one or two places per swine at the normal posterior lobe of lung, or 10 places in total. A set of 40 thermocouples located around the cryoprobe were used for temperature measurement. A temperature simulation model is proposed and thereby allows real-time monitoring of the temperature behavior during a treatment of cryoablation. Moreover, the freeze-thaw sequence was analyzed by using the freezing function indicated in Eq. (1).

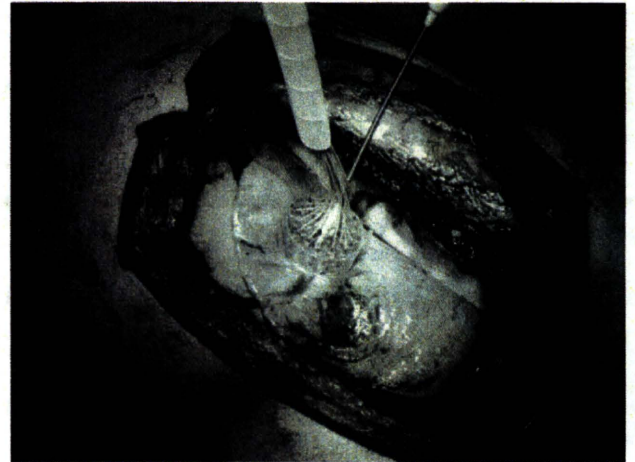


Fig. 3. The picture showing how the temperature is measured. Cryoprobe and thermocouples are inserted by pressing the measurement device to the posterior lobe of lung.

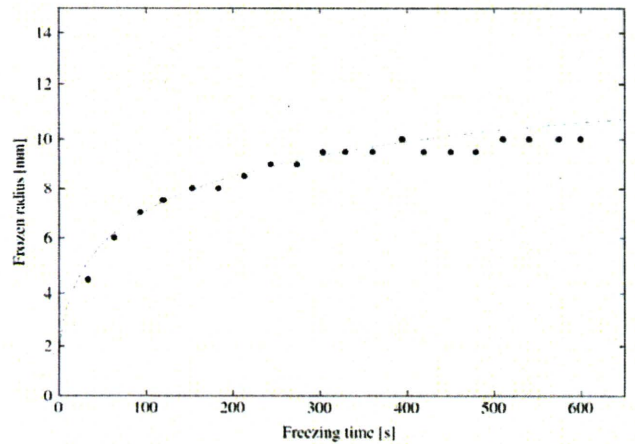


Fig. 4. Comparison of the frozen radius between the experimental data (dot) and the analytical solution (line). Freezing curve by the analytical solution is calculated by using the parameter set 2 in Table 3 except $\omega_{eff} = 0.04$. The experimental data originate from [8].

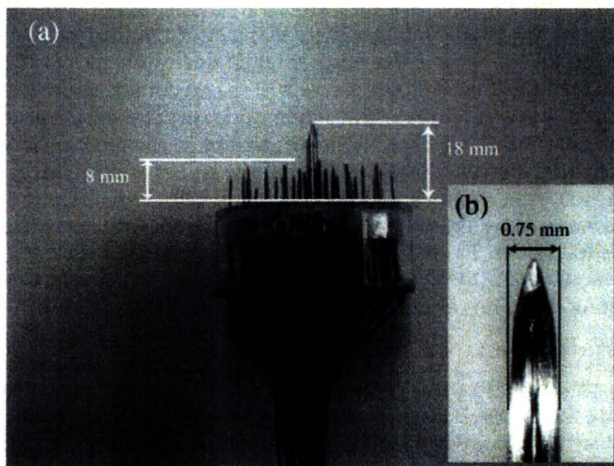


Fig. 2. (a) The cryoprobe and the measurement device. The cryoprobe at the center and the thermocouples are fixed at 18 and 8 mm from the tip of each for the depth of puncture in the porcine lung. (b) The tip of a thermocouple. The alumel wire and the chromel wire are connected only at the tip.



Fig. 5. Bleeding around the cryoprobe at the first thawing. The freeze-thaw cycle was completed three times at the other bleeding spot below.